Simple approach to fourth generation effects in B>Xsl+l− decay

Article *in* Physical review D: Particles and fields · January 2004

DOI: 10.1103/PhysRevD.69.015003 · Source: arXiv

1 author:

Levent Solmaz
Balikesir University
26 PUBLICATIONS **82** CITATIONS

A Simple Approach to Fourth Generation Effects in $B \to X_s \ell^+ \ell^-$ Decay

Levent Solmaz*
Balikesir University, Physics Department (32), Balikesir, Turkey
(Dated: February 7, 2008)

Abstract

In a scenario in which fourth generation fermions exist, we study effects of new physics on the differential decay width, forward-backward asymmetry and integrated branching ratio for $B \to X_s \ell^+ \ell^-$ decay with $(\ell = e, \mu)$. Prediction of the new physics on the mentioned quantities essentially differs from the Standard Model results, in certain regions of the parameter space, enhancement of new physics on the above mentioned physical quantities can yield values as large as two times of the SM predictions, whence present limits of experimental measurements of branching ratio is spanned, contraints of the new physics can be extracted. For the fourth generation CKM factor $V_{t'b}^* V_{t's}$ we use $\pm 10^{-2}$ and $\pm 10^{-3}$ ranges, take into consideration the possibility of a complex phase where it may bring sizable contributions, obtained no significant dependency on the imaginary part of the new CKM factor. For the above mentioned quantities with a new family, deviations from the SM are promising, can be used as a probe of new physics.

*Electronic address: lsolmaz@photon.physics.metu.edu.tr,lsolmaz@balikesir.edu.tr

I. INTRODUCTION

Even if Standard Model (SM) is a successful theory, one should also check probable effects that may come from potential new physics. In the SM, since we do not have a clear theoretical argument to restrict number of generations to three, possibility of a new generation should not be ruled out until there is a certain evidence which order us to do so. This is especially true for rare B decays, which are very sensitive to generic expansions of the SM, due to their loop structure. We know from neutrino experiments that, for the mass of the extra generations there is a lower bound for the new generations ($m_{\nu_4} > 45\ GeV$) [1]. Probable effects of extra generations was studied in many works [2]–[16]. The existing electroweak data on the Z–boson parameters, the W boson and the top quark masses excluded the existence of the new generations with all fermions heavier than the Z boson mass [16], nevertheless, the same data allows a few extra generations, if one allows neutral leptons to have masses close to 50 GeV. In addition to this, recently observed neutrino oscillations requires an enlarged neutrino sector [17].

Generalizations of the SM can be used to introduce a new family, which was performed previously [18]. Using similar techniques, one can search fourth generation effects in B meson decays. The contributions from fourth generation to rare decays have been extensively studied [19, 20, 21, 22, 23], where the measured decay rate has been used to put stringent constraints on the additional CKM matrix elements. In addition to $B \to X_s\gamma$, $B \to X_s\ell^+\ell^-$ can be mentioned as one of the most promising areas in search of the fourth generation, via its indirect loop effects, to constrain $V^*_{t'b}V_{t's}$ [24, 25]. The restrictions of the parameter space of nonstandard models based on LO analysis are not as sensitive as in the case of NLO analysis, hence a NLO analysis considering the possibility of a complex phase is important, which we plan to revise [26].

On the experimental side, the inclusive $B \to X_s\ell^+\ell^-$ (with $\sqrt{q^2} > 0.2$ GeV) decay with electron and muon modes combined ($\ell = e, \mu$) have been observed (Belle [27]), (BaBar [28]),

$$\mathcal{B}(B \to X_s\ell^+\ell^-) = (6.1 \pm 1.4^{+1.4}_{-1.1}) \cdot 10^{-6}, \tag{1}$$

$$\mathcal{B}(B \to X_s\ell^+\ell^-) = (6.3 \pm 1.6^{+1.8}_{-1.5}) \cdot 10^{-6}\ . \tag{2}$$

They are in agreement with the SM $\mathcal{B}(B \to X_s\ell^+\ell^-)_{SM} = 4.2 \pm 0.7 \cdot 10^{-6}$ for the same cuts [29].

On the theoretical side, situation within and beyond the SM is well settled. A collective theoretical effort has led to the practical determination of $B \to X_s\ell^+\ell^-$ at the NNLO, which was completed recently, as a joint effort of different groups ([30, 31, 32]), and references therein. It is necessary to have precise calculations also in the extensions of the SM, which was performed for certain models. With the appearance of more accurate data we might be able to provide stringent constrains on the free parameters of the models beyond SM. From this respect, a NNLO analysis of the new generation is important. We study the contribution of the fourth generation in the rare $B \to X_s\ell^+\ell^-$decay at NNLO, to obtain experimentally measurable quantities which is expected to appear in the forthcoming years.

The paper is organized as follows. In section 2, we present the necessary theoretical expressions for the $B \to X_s\ell^+\ell^-$decay in the SM with four generations. Section 3 is devoted to our conclusion.

II. $B \to X_S\ell^+\ell^-$ DECAY AND FOURTH GENERATION

We use the framework of an effective low-energy theory, obtained by integrating out heavy degrees of freedoms, which in our case W-boson and top quark and an additional t' quark. Mass of the t' is at the order of μ_W. In this approximation the effective Hamiltonian relevant for the $B \to X_s\ell^+\ell^-$decay reads [33]

$$\mathcal{H}_{\text{eff}} = -\frac{4G_F}{\sqrt{2}} V^*_{ts}V_{tb} \sum_{i=1}^{10} C_i(\mu)\, O_i(\mu) \quad , \tag{3}$$

where G_F is the Fermi coupling constant V is the Cabibbo-Kobayashi-Maskawa (CKM) quark mixing matrix, the the full set of the operators $O_i(\mu)$ and the corresponding expressions for the Wilson coefficients $C_i(\mu)$ in the SM can be found in Ref.[30].

In the model under consideration, the fourth generation is introduced in a similar way the three generations are introduced in the SM, no new operators appear and clearly the full operator set is exactly the same as in SM, which is a rough approximation. The fourth generation changes values of the Wilson coefficients $C_i(\mu)$, $i = 7, 8, 9$ and 10, via virtual exchange of the fourth generation up quark t'. With the definitions $\lambda_j = V^*_{js}V_{jb}$, where $j = u,\ c,\ t,\ t'$, the new physics Wilson coefficients can be written in the following form

$$C_i^{4G}(\mu_W) = \frac{\lambda_{t'}}{\lambda_t} C_i(\mu_W)_{m_t \to m_{t'}}\ , \tag{4}$$

where the last terms in these expression describes the contributions of the t' quark to the Wilson coefficients with the replacement of m_t with $m_{t\prime}$. Notice that we use the definition $\lambda_{t'} = V^*_{t's}V_{t'b}$ which is the element of the 4×4 Cabibbo–Kobayashi–Maskawa (CKM) matrix, from now on '4G' will stand for sequential fourth generation model. In this model properties of the new t' quark are the same as ordinary t, except its mass and corresponding CKM couplings. A few comments are in order here: to obtain quantitative results we need the value of the fourth generation CKM matrix element $V^*_{t's}V_{tb}$ which can be extracted i.e. from $B \to X_s\gamma$ decay as a function of mass of the new top quark m'_t. For this aim following [24, 25], we can use the fourth generation CKM factor $\lambda_{t'}$ in the range $-10^{-2} \leq \lambda_{t'} \leq 10^{-2}$. In the numerical analysis, as a first step, $\lambda_{t'}$ is assumed real and expressions are obtained as a function of mass of the extra generation top quark $m_{t'}$. It is interesting to notice that, if we assume $\lambda_{t'}$ can have imaginary parts, experimental values can also be satisfied [23, 26]. Nevertheless, if we impose the unitarity condition of the CKM matrix we have

$$V^*_{us}V_{ub} + V^*_{cs}V_{cb} + V^*_{ts}V_{tb} + V^*_{t's}V_{t'b} = 0\ . \tag{5}$$

With the values of the CKM matrix elements in the SM [34], the sum of the first three terms in Eq. (5) is about 7.6×10^{-2}, where the error in sum of first three terms is about $\pm0.6\times10^{-2}$. We assume the value of $\lambda_{t'}$ is within this error range.

What should not be ignored in constraining $\lambda_{t'}$ is that, when adding a fourth family the present constrains on the elements of CKM may get relaxed [34]. In order to have a clear picture of $\lambda_{t'}$, CKM matrix elements should be calculated with the possibility of a new family, using present experiments that constitutes the CKM. From this respect we do not have to exclude certain regions that violate unitarity of the present CKM, but take it in the ranges $-10^{-2} \leq \lambda_{t'} \leq 10^{-2}$ and $-10^{-3} \leq \lambda_{t'} \leq 10^{-3}$.

A. Differential Decay Width

Since extended models are very sensitive to NNLO corrections, we used the NNLO expression for the branching ratio of the radiative decay $B \to X_s\ell^+\ell^-$, which has been presented in Refs. [29, 33]. In the NNLO approximation, the invariant dilepton mass distribution for the inclusive decay $B \to X_s\ell^+\ell^-$ can be written as

$$\begin{aligned}\frac{d\Gamma(b\to X_s\ell^+\ell^-)}{d\hat{s}} &= \left(\frac{\alpha_{em}}{4\pi}\right)^2 \frac{G_F^2 m_{b,pole}^5 \left|V^*_{ts}V_{tb}\right|^2}{48\pi^3}(1-\hat{s})^2 \\ &\times\left((1+2\hat{s})\left(\left|\widetilde{C}_9^{\rm eff}\right|^2+\left|\widetilde{C}_{10}^{\rm eff}\right|^2\right)+4\,(1+2/\hat{s})\left|\widetilde{C}_7^{\rm eff}\right|^2+12{\rm Re}\left(\widetilde{C}_7^{\rm eff}\widetilde{C}_9^{\rm eff*}\right)\right)\ ,\end{aligned} \tag{6}$$

where $\hat{s} = m^2_{\ell^+\ell^-}/m^2_{b,pole}$ with ($\ell = e$ or μ). In the SM the effective Wilson coefficients $\tilde{C}_7^{\rm eff}$, $\tilde{C}_9^{\rm eff}$ and $\tilde{C}_{10}^{\rm eff}$ are given by [30, 33] and can be obtained from Eqs.(8,9 and 10), by setting $4G \to\ 0$. Following the lines of A.Ali [29] with the assumption that only the lowest non-trivial order of these Wilson coefficients get modified by new physics, which means that $C_7^{(1)}(\mu_W)$, $C_8^{(1)}(\mu_W)$, $C_9^{(1)}(\mu_W)$ and $C_{10}^{(1)}(\mu_W)$ get modified, the shifts of the Wilson coefficients at μ_W can be written as

$$C_i(\mu_W) \longrightarrow C_i(\mu_W) + \frac{\alpha_s}{4\pi}\,C_i^{4G}(\mu_W)\,. \tag{7}$$

These shift at the matching scale are resulted in the modifications of the effective Wilson coefficients,

$$\begin{aligned}\widetilde{C}_7^{\rm eff} &= \left(1+\frac{\alpha_s(\mu)}{\pi}\omega_7(\hat{s})\right)\left(A_7 + A_{77}\,C_7^{4G}(\mu_W) + A_{78}\,C_8^{4G}(\mu_W)\right) \\ &\quad -\frac{\alpha_s(\mu)}{4\pi}\left(C_1^{(0)}F_1^{(7)}(\hat{s}) + C_2^{(0)}F_2^{(7)}(\hat{s}) + A_8^{(0)}F_8^{(7)}(\hat{s}) + A_{88}^{(0)}\,C_8^{4G}(\mu_W)\,F_8^{(7)}(\hat{s})\right)\ ,\end{aligned} \tag{8}$$

$$\begin{aligned}\widetilde{C}_9^{\rm eff} &= \left(1+\frac{\alpha_s(\mu)}{\pi}\omega_9(\hat{s})\right)\left(A_9 + T_9\,h(\hat{m}_c^2,\hat{s}) + U_9\,h(1,\hat{s}) + W_9\,h(0,\hat{s}) + C_9^{4G}(\mu_W)\right) \\ &\quad -\frac{\alpha_s(\mu)}{4\pi}\left(C_1^{(0)}F_1^{(9)}(\hat{s}) + C_2^{(0)}F_2^{(9)}(\hat{s}) + A_8^{(0)}F_8^{(9)}(\hat{s}) + A_{88}^{(0)}\,C_8^{4G}(\mu_W)\,F_8^{(9)}(\hat{s})\right)\ ,\end{aligned} \tag{9}$$

$$\widetilde{C}_{10}^{\rm eff} = \left(1+\frac{\alpha_s(\mu)}{\pi}\omega_9(\hat{s})\right)\left(A_{10} + C_{10}^{4G}\right). \tag{10}$$

The numerical values for the parameters A_{77}, A_{78}, $A_{88}^{(0)}$, which incorporate the effects from the running, can be found in the same reference [29], for the functions $h(\hat{m}_c^2,\hat{s})$ and $\omega_9(\hat{s})$, they are given in Ref. [30], while $\omega_7(\hat{s})$ and $F_{1,2,8}^{(7,9)}(\hat{s})$

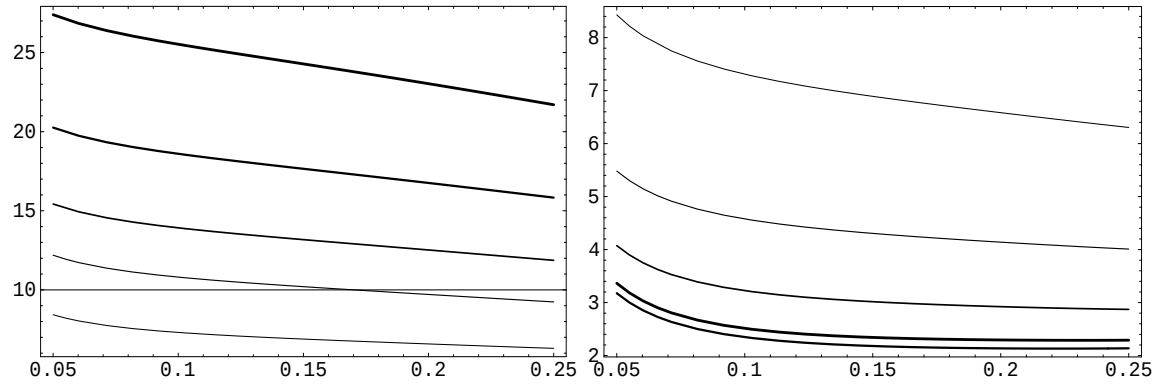

FIG. 1: Branching ratio $\mathcal{B}^{B\to X_s\ell^+\ell^-}$ $[10^{-6}]$ as a function of $\hat{s}\in[0.05,0.25]$(see Eq.(11)). The four thick lines show the NNLL prediction for $m_{t\prime}=200,300,400$ and 500 with increasing thickness respectively and the SM prediction is the thin line. The figures are obtained at the scale $\mu=5.0\ GeV$. For the figure at the Left: $\lambda_{t\prime}=-10^{-2}$, Right: $\lambda_{t\prime}=10^{-2}$.

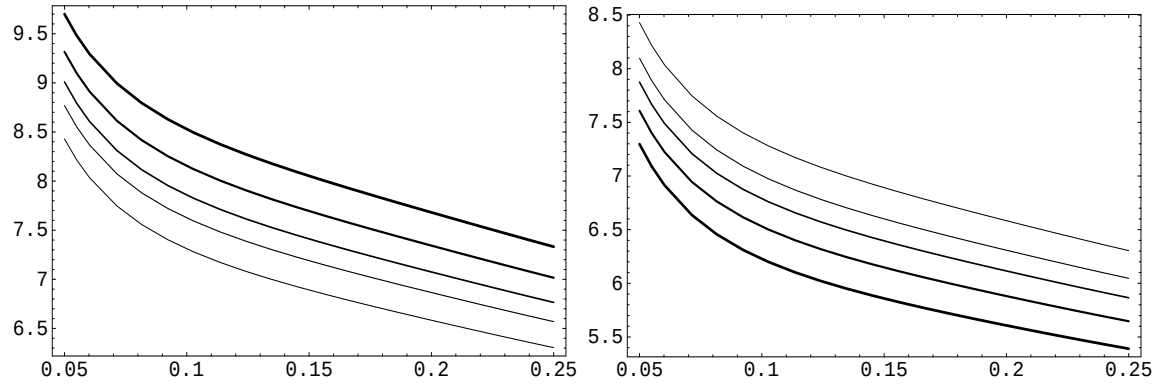

FIG. 2: The same as Fig.1 with the choices, For the figure at the Left: $\lambda_{t\prime}=-10^{-3}$, Right: $\lambda_{t\prime}=10^{-3}$

can be seen in Ref. [33]. In order to remove the large uncertainty coming from m_b terms it is customary to use the following expression [29]

$$\mathcal{B}^{B\to X_s\ell^+\ell^-}(\hat{s})=\frac{\mathcal{B}^{B\to X_ce\bar{\nu}}_{\rm exp}}{\Gamma(B\to X_ce\bar{\nu})}\frac{d\Gamma(B\to X_s\ell^+\ell^-)}{d\hat{s}}\,, \tag{11}$$

which can be called as branching ratio. The explicit expression for the semi-leptonic decay width can be found in Ref. [30]. The branching ratio with 4G is presented in Figs. (1,2) for the choice of the scale $\mu=5\ GeV$.

In the figures related with dilepton invariant mass distribution we used the low region $\hat{s}\in[0.05,0.25]$ where peaks stemming from $c\bar{c}$ resonances are expected to be small. During the calculations we take $\mathcal{B}^{B\to X_ce\bar{\nu}}_{\rm exp}=0.1045$.

B. Forward-Backward asymmetry

We investigate both, the so-called normalized and the unnormalized forward-backward asymmetry with 4G model. The double differential decay width $d^2\Gamma(b\to X_s\ell^+\ell^-)/(d\hat{s}\,dz)$, $(z=\cos(\theta))$ is expressed as [31]

$$\frac{d^2\Gamma(b\to X_s\,\ell^+\ell^-)}{d\hat{s}\,dz}=\quad\Big(\frac{\alpha_{em}}{4\,\pi}\Big)^2\,\frac{G_F^2\,m_{b,\rm pole}^5\,|V_{ts}^*V_{tb}|^2}{48\,\pi^3}(1-\hat{s})^2$$

$$
\begin{aligned}
&\times \left\{ \frac{3}{4}[(1-z^2)+\hat{s}(1+z^2)] \left(\left|\widetilde{C}_9^{\rm eff}\right|^2 + \left|\widetilde{C}_{10}^{\rm eff}\right|^2 \right) \left(1+\frac{2\alpha_s}{\pi} f_{99}(\hat{s},z)\right) \right. \\
&+\frac{3}{\hat{s}}[(1+z^2)+\hat{s}(1-z^2)] \left|\widetilde{C}_7^{\rm eff}\right|^2 \left(1+\frac{2\alpha_s}{\pi} f_{77}(\hat{s},z)\right) \\
&-3\,\hat{s}\,z\,{\rm Re}(\widetilde{C}_9^{\rm eff}\widetilde{C}_{10}^{\rm eff*}) \left(1+\frac{2\alpha_s}{\pi} f_{910}(\hat{s})\right) \\
&+6\,{\rm Re}(\widetilde{C}_7^{\rm eff}\widetilde{C}_9^{\rm eff*}) \left(1+\frac{2\alpha_s}{\pi} f_{79}(\hat{s},z)\right) \\
&\left. -6\,z\,{\rm Re}(\widetilde{C}_7^{\rm eff}\widetilde{C}_{10}^{\rm eff*}) \left(1+\frac{2\alpha_s}{\pi} f_{710}(\hat{s})\right) \right\} . \qquad (12)
\end{aligned}
$$

where θ is the angle between the momenta of the b quark and the ℓ^+, measured in the rest frame of the lepton pair. The functions $f_{99}(\hat{s},z)$, $f_{77}(\hat{s},z)$, $f_{910}(\hat{s})$, $f_{79}(\hat{s},z)$ and $f_{710}(\hat{s})$ are the analogues of $\omega_{99}(\hat{s})$, $\omega_{77}(\hat{s})$ and $\omega_{79}(\hat{s})$ which can be found in the same reference [31]

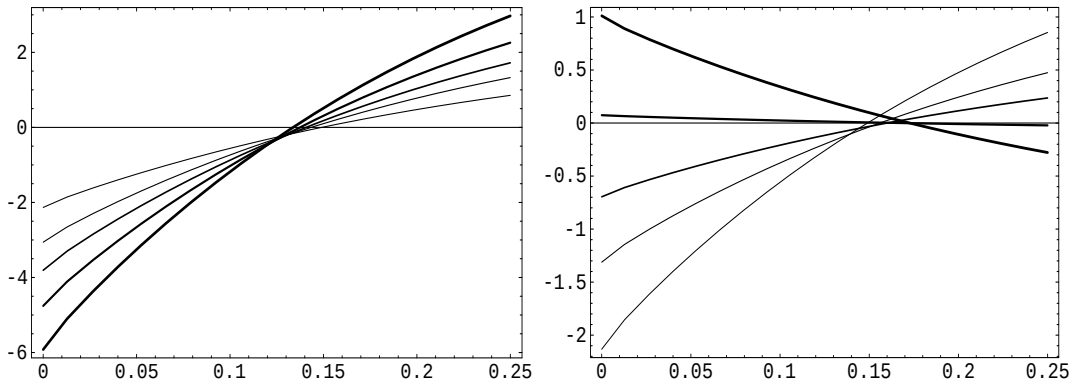

FIG. 3: Unnormalized forward-backward asymmetry $A_{\rm FB}$ $[10^{-6}]$ as a function of $\hat{s} \in [0, 0.25]$ (see Eq.(13)). The four thick lines show the NNLL prediction for $m_{t\prime} = 200, 300, 400$ and 500 with increasing thickness respectively and the SM prediction is the thin line. The figures are obtained at the scale $\mu = 5.0\ GeV$. For the figure at the Left: $\lambda_{t\prime} = -10^{-2}$, Right: $\lambda_{t\prime} = 10^{-2}$.

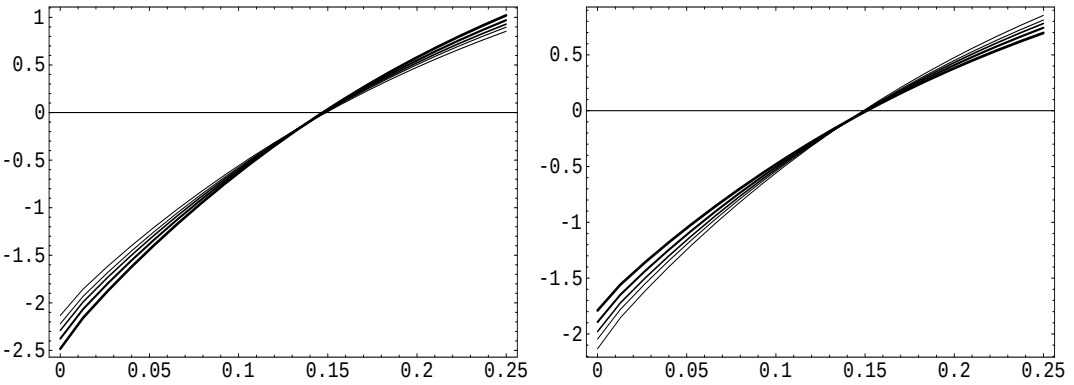

FIG. 4: The same as Fig.3 with the choices: Left: $\lambda_{t\prime} = -10^{-3}$, Right: $\lambda_{t\prime} = 10^{-3}$

The unnormalized version of forward-backward asymmetry, $A_{\rm FB}(\hat{s})$ is defined as

$$
A_{\rm FB}(\hat{s}) \;=\; \frac{\int_{-1}^{1} \frac{d^2\Gamma(b\to X_s\,\ell^+\ell^-)}{d\hat{s}\,dz}\,{\rm sgn}(z)\,dz}{\Gamma(B\to X_c e\bar{\nu}_e)}\,\mathcal{B}_{\rm exp}^{B\to X_c e\bar{\nu}}\,, \qquad (13)
$$

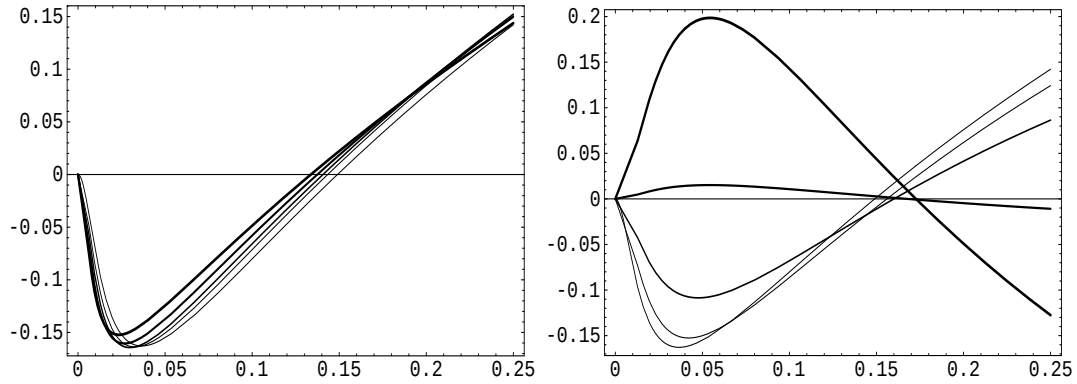

FIG. 5: Normalized forward-backward asymmetry $\overline{A}_{\rm FB}$ $[10^{-6}]$ as a function of $\hat{s} \in [0, 0.25]$ (see Eq.(14)). The four thick lines show the NNLL prediction for $m_{t\prime} = 200, 300, 400$ and 500 with increasing thickness respectively and the SM prediction is the thin line. The figures are obtained at the scale $\mu = 5.0\ GeV$. For the figure at the Left: $\lambda_{t\prime} = -10^{-2}$, Right: $\lambda_{t\prime} = 10^{-2}$.

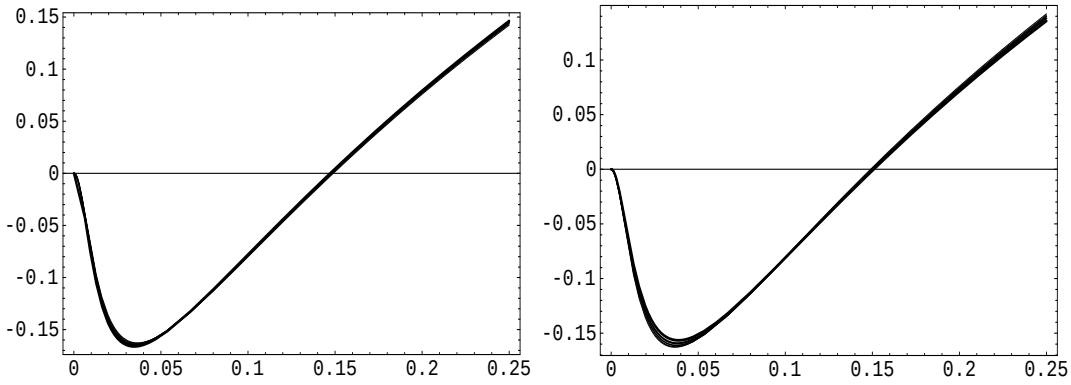

FIG. 6: The same as Fig.5 with the choices: Left: $\lambda_{t\prime} = -10^{-3}$, Right: $\lambda_{t\prime} = 10^{-3}$.

while the definition of the normalized forward-backward asymmetry $\overline{A}_{\rm FB}(\hat{s})$ reads

$$\overline{A}_{\rm FB}(\hat{s}) \;=\; \frac{\int_{-1}^{1} \frac{d^2\Gamma(b\to X_s\,\ell^+\ell^-)}{d\hat{s}\,dz}\,{\rm sgn}(z)\,dz}{\int_{-1}^{1} \frac{d^2\Gamma(b\to X_s\,\ell^+\ell^-)}{d\hat{s}\,dz}\,dz}\,. \tag{14}$$

The position of the zero of the $A_{FB}(\hat{s}_0) = 0$ is very sensitive to 4G effects as it is seen in the figures (3,5). However as 4G parameter $\lambda_{t'}$ decreases expectations of the new model are getting closer to SM values which can be inferred from Figs.(4,6)

C. Integrated Branching Ratio

By suitable choice of integration limits over $\hat{s}$ one can obtain integrated branching ratio in accordance with the experiment for e and μ, which is already performed, hence we use the integrated branching ratio expression which has the following form [29]:

$$\begin{aligned}\mathcal{B}(B\to X_s\ell^+\ell^-) \;=\; & 10^{-6}\times\Big[a_1 + a_2\,|A_7^{\rm tot}|^2 + a_3\,(|C_9^{\rm 4G}|^2 + |C_{10}^{\rm 4G}|^2)\\ & + a_4\,{\rm Re}\,A_7^{\rm tot}\,{\rm Re}\,C_9^{\rm 4G} + a_5\,{\rm Im}\,A_7^{\rm tot}\,{\rm Im}\,C_9^{\rm 4G} + a_6\,{\rm Re}\,A_7^{\rm tot}\\ & + a_7\,{\rm Im}\,A_7^{\rm tot} + a_8\,{\rm Re}\,C_9^{\rm 4G} + a_9\,{\rm Im}\,C_9^{\rm 4G} + a_{10}\,{\rm Re}\,C_{10}^{\rm 4G}\Big]\,,\end{aligned} \tag{15}$$

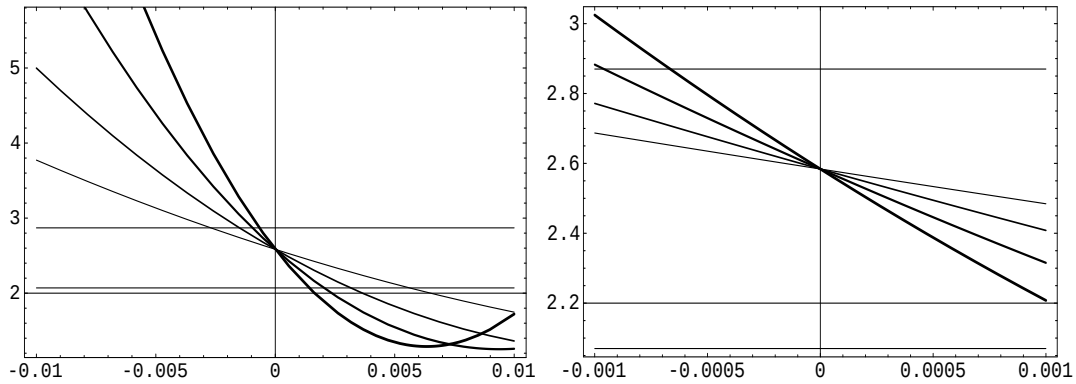

FIG. 7: Integrated Branching ratio B($B \to X_s \ell^+ \ell^-$) $[10^{-6}]$ as a function of $\lambda_{t\prime}$ for $\ell = e$ (see Eq.(15)). In the left figure $\lambda_{t\prime} \in [-10^{-2}, 10^{-2}]$. For the figure at the right $\lambda_{t\prime} \in [-10^{-3}, 10^{-3}]$. In the figures straight lines shows the SM allowed region.

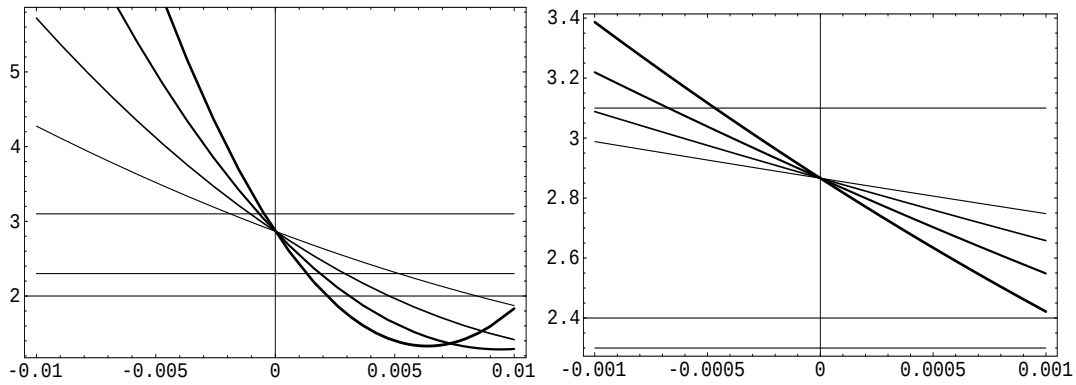

FIG. 8: Integrated Branching ratio B($B \to X_s \ell^+ \ell^-$) $[10^{-6}]$ as a function of $\lambda_{t\prime}$ for $\ell = \mu$. In the left figure $\lambda_{t\prime} \in [-10^{-2}, 10^{-2}]$. For the figure at the right $\lambda_{t\prime} \in [-10^{-3}, 10^{-3}]$. In the figures straight lines show the SM region.

where the numerical value of the coefficients a_i are given in Table I for $\ell = e,\ \mu$. For the integrated branching ratios we refer to Figs.(7,8) of electron and muon respectively.

ℓ	a_1	a_2	a_3	a_4	a_5	a_6	a_7	a_8	a_9	a_{10}
e	1.9927	6.9357	0.0640	0.5285	0.6574	0.2673	-0.0586	0.4884	0.0095	-0.5288
μ	2.3779	6.9295	0.0753	0.6005	0.7461	0.5955	-0.0600	0.5828	0.0102	-0.6225

TABLE I: Numerical values of the coefficients a_i (evaluated at $\mu_b = 5$ GeV) for the decays $B \to X_s \ell^+ \ell^-$ ($\ell = e,\ \mu$), taken from Ref. [29].

III. DISCUSSION

In the sequential fourth generation model, there are basically two free parameters, mass of new generations and CKM factors which can have imaginary phases. As a worst scenario, we decompose $\lambda_{t\prime} = Re[\lambda_{t\prime}] + I \times Im[\lambda_{t\prime}]$ and choose the range $\frac{Im[\lambda_{t\prime}]}{Re[\lambda_{t\prime}]} \leq 10^{-2}$; we checked the effect of this choice and observe that contribution from the imaginary

part can be neglected for all of the kinematical observables. Naturally, these quantities should be fixed by respecting experiment. Besides, constraints for CKM values should be updated by noting that existance of a new generation can relax the matrix elements of $\mathrm{CKM}_{3\times3}$, when it is accepted as a sub-matrix of $\mathrm{CKM}_{4\times4}$.

Since scale dependency of NNLO calculations of $B \to X_s\ell^+\ell^-$ are not very high [31], during the calculations we set the scale $\mu = 5\ GeV$, use the main input parameters as follows,

$$\begin{aligned} \alpha_{em} &= 1/133\,, \alpha_s(m_Z) = 0.119\,, G_F = 1.16639\times10^{-5}\,\mathrm{GeV}^{-2}\,, m_W = 80.33\,\mathrm{GeV}\,, \\ m_b &= 4.8\,\mathrm{GeV}\,, m_t = 176\,\mathrm{GeV},\ m_c = 1.4\,\mathrm{GeV},\ \text{Wolfenstein parameters:} \\ A &= 0.75\,, \lambda = 0.221\,, \rho = 0.4, \eta = 0.2\,. \end{aligned} \tag{16}$$

Effects of new physics on kinemaical observables can be summerized as follows:

- Differential decay width $\mathcal{B}^{B\to X_s\ell^+\ell^-}$ is presented in figures Fig.(1,2), where it is shown that SM prediction can be strongly enhanced with a new quark for the choice $\lambda_{t\prime} < 0$. It is also possible to supress the decay width for positive solutions of $\lambda_{t'}$ which is not favored.

- Forward-Backward asymmetry is also very sensitive to 4G effects, especially for the choice $\lambda_{t\prime} = 10^{-2}$. As it is seen in Figs.(3,5), as the mass of $m_{t'}$ increases it is even possible to have positive values for $A_{FB}(0)$ which is in contradiction with SM, but natural in extended models. Once the experimental results related with this quantity is obtained, it will be a keen test of fourth generation model. Deviations from the point $\hat{s}$=0 are detectable as it is seen in Fig.(4) for the choice of $\lambda_{t\prime} \in [-10^{-3}, 10^{-3}]$, whereas for the same region we see almost no dependence on the normalized forward-backward asymmetry in Fig.(6). While Standard Model states the central value $A_{\mathrm{FB}}^{\mathrm{NNLO}}(0) = -(2.30 \pm 0.10)\times10^{-6}$, 4G predictions cover the range $A_{\mathrm{FB}}^{\mathrm{4G,NNLO}}(0) \in [-6, 1]\times10^{-6}$for the choices $\lambda_{t'} = -10^{-2}, 10^{-2}$ respectively. For the point where forward-backward asymmetry vanishes Standard Model result is $\hat{s}_0^{\mathrm{NNLO}} = 0.162 \pm 0.002$ however 4G predictions are roughly $\hat{s}_0^{\mathrm{4G,NNLO}} \in [0.13, 0.18]$.

- Integrated branching ratios Figs.(7,8) strongly depends on the new physics parameters $\lambda_{t\prime}$ and $m_{t'}$, therefore it is possible to restrict them by respecting experiments. As it can be deduced from the figures when 4G effects are switched off our calculations are lying on the SM ground within error bars [29]. Similar to branching ratio for integrated branching ratios enhancement comes from negative choices of $\lambda_{t'}$ which favors smaller values for $A_{\mathrm{FB}}^{\mathrm{SM,NNLO}}(0) = -(2.30 \pm 0.10)\times10^{-6}$.

To summarize, in this work we present the predictions of the sequential fourth generation model for experimentally measurable quantities related with $B \to X_s\ell^+\ell^-$ decay which is expected to emerge in the near future thanks to running B factories. These predictions differ from SM in certain regions, hence can be used, to differentiate the existence of the fourth family or to put stringent constrains on the free parameters of the model, if it exists.

[1] P. Abreu et al., (DELPHI Collaboration), Phys. Lett. **B274** (1992) 23.
[2] X. G. He and S. Paksava, Nucl. Phys. **B278** (1986) 905.
[3] A. Anselm et al., Phys. Lett. **B156** (1985) 103.
[4] U. Turke et al., Nucl. Phys. **B258** (1985) 103.
[5] I. Bigi, Z. Phys. **C27** (1985) 303.
[6] G. Eilam, J. L. Hewett and T. G. Rizzo, Phys. Rev. **D34** (1986) 2773.
[7] W. S. Hou and R. G. Stuart, Phys. Rev. **D43** (1991) 3669.
[8] N. G. Deshpande, J. Trampetic, Phys. Rev. **D40** (1989) 3773.
[9] G. Eilam, B. Haeri and A. Soni, Phys. Rev. **D41** (1990) 875; Phys. Rev. Lett. **62** (1989) 719.
[10] N. Evans, Phys. Lett. **B340** (1994) 81.
[11] P. Bamert and C. P. Burgess, Z. Phys. **C66** (1995) 495.
[12] T. Inami et al., Mod. Phys. Lett. **A10** (1995) 1471.
[13] A. Masiero et al., Phys. Lett. **B355** (1995) 329.
[14] V. Novikov, L. B. Okun, A. N. Rozanov et al., Mod. Phys. Lett. **A10** (1995) 1915; Erratum. ibid **A11** (1996) 687; Rep. Prog. Phys. **62** (1999) 1275.
[15] J. Erler, P. Langacker, Eur. J. Phys. **C3** (1998) 90.
[16] M. Maltoni et al., prep. [hep–ph/9911535 (1999)].
[17] P.H. Frampton, P.Q. Hung and M. Sher, Phys. Rept. **330**, 263 (2000); J.I. Silva-Marcos, [hep-ph/0204217].
[18] J. F. Gunion, D. McKay and H. Pois, Phys. Rev. **D51** (1995) 201;
[19] W.S. Hou, A. Soni and H. Steger, Phys. Lett. B **192**, 441 (1987).
[20] W.S. Hou, R.S. Willey and A. Soni, Phys. Rev. Lett. **58**, 1608 (1987) [Erratum-ibid. **60**, 2337 (1987)].

[21] T. Hattori, T. Hasuike and S. Wakaizumi, Phys. Rev. D **60**, 113008 (1999); T.M. Aliev, D.A. Demir and N.K. Pak, Phys. Lett. B **389**, 83 (1996) Y. Dincer, Phys. Lett. B **505**, 89 (2001) and references therin.
[22] C.S. Huang, W.J. Huo and Y.L. Wu, Mod. Phys. Lett. A **14**, 2453 (1999) C.S. Huang, W.J. Huo and Y.L. Wu, Phys. Rev. D **64**, 016009 (2001)
[23] T.M. Aliev, A. Özpineci and M. Savcı, Eur.Phys.J. C 29 (2003) 265-270 [hep-ph/0301078]
[24] C. S. Huang, W. J. Huo and Y. L. Wu, prep. [hep–ph/9911203] (1999).
[25] T. M. Aliev et al., Nucl. Phys. B. **585** (2000) 275.
[26] L. Solmaz, [hep–ph/0204016] (2002).
[27] J. Kaneko et al. [Belle Collaboration], Phys. Rev. Lett. **90**, 021801 (2003) [hep-ex/0208029].
[28] B. Aubert [BABAR Collaboration], [hep-ex/0308016].
[29] A. Ali et al., Phys. Rev. D **66**, 034002 (2002) [hep-ph/0112300].
[30] C. Bobeth, M. Misiak and J. Urban, Nucl. Phys. B **574** (2000) 291 [hep-ph/9910220].
[31] H. M. Asatrian et al., Phys. Rev. D **66**, 094013 (2002) [hep-ph/0209006].
[32] A. Ghinculov et al., Nucl. Phys. B **648**, 254 (2003) [hep-ph/0208088];
[33] H. H. Asatrian, H. M. Asatrian, C. Greub and M. Walker, Phys. Lett. B **507** (2001) 162 [hep-ph/0103087];
H. H. Asatryan, H. M. Asatrian, C. Greub and M. Walker, Phys. Rev. D **65** (2002) 074004 [hep-ph/0109140].
[34] C. Caso et al., Eur. J. Phys. **C3** (1998) 1.